

Strong Dynamo Action in Rapidly Rotating Suns

Benjamin P. Brown^{*}, Matthew K. Browning[†], Allan Sacha Brun^{**}, Mark S. Miesch[‡], Nicholas J. Nelson^{*} and Juri Toomre^{*}

^{*}*JILA and Dept. of Astrophysical & Planetary Sciences, University of Colorado, Boulder, CO 80309-0440*

[†]*Dept. of Astronomy, University of California, Berkeley, CA 94720-3411*

^{**}*DSM/DAPNIA/SAP, CEA Saclay, Gif sur Yvette, 91191 Cedex, France*

[‡]*High Altitude Observatory, NCAR, Boulder, CO 80307-3000*

Abstract. Stellar dynamos are driven by complex couplings between rotation and turbulent convection, which drive global-scale flows and build and rebuild stellar magnetic fields. When stars like our sun are young, they rotate much more rapidly than the current solar rate. Observations generally indicate that more rapid rotation is correlated with stronger magnetic activity and perhaps more effective dynamo action. Here we examine the effects of more rapid rotation on dynamo action in a star like our sun. We find that vigorous dynamo action is realized, with magnetic field generated throughout the bulk of the convection zone. These simulations do not possess a penetrative tachocline of shear where global-scale fields are thought to be organized in our sun, but despite this we find strikingly ordered fields, much like sea-snakes of toroidal field, which are organized on global scales. We believe this to be a novel finding.

Keywords: convection – magnetohydrodynamics – stars:interior, rotation, dynamo action – differential rotation

PACS: 47.27.ep; 95.30.Qd; 97.10.Kc; 97.10.Ld; 97.20.Jg

1. Coupling of convection, rotation and magnetism

Rotation and convection are key components of stellar dynamo action. It is their complex coupling which must lead to the global-scale fields observed in our sun and other solar-like stars. When stars like our sun are young they rotate much more rapidly than the current solar rate. Observations generally indicate that more rapid rotation is correlated with stronger magnetic activity, which may indicate a stronger stellar dynamo. Here we explore the effects of more rapid rotation on convection and dynamo action in a more rapidly rotating solar-like star.

In the sun, global-scale dynamo action is thought to arise from the coupling of convection and rotation and the resulting global-scale flows of differential rotation and meridional circulation. As revealed by helioseismology, the solar differential rotation profile observed at the surface prints throughout the bulk of the convection zone, with two prominent regions of radial shear. The near-surface shear layer exists in the outer 5% of the sun, whereas the tachocline lies between the radiative interior, which is in nearly solid body rotation, and the convective envelope above (Thompson et al., 2003). In the interface dynamo model (e.g., Charbonneau, 2005), magnetic fields generated in the bulk of the convection zone are pumped into the stably stratified tachocline where the strong radial shear builds and organizes the global-scale fields that eventually erupt at the solar surface. The differential rotation plays an important role in the production of

the global-scale magnetic fields while the meridional circulations may be important for returning flux to the base of the convection zone, enabling cycles of magnetic activity. In observations of solar-like stars the differential rotation appears to grow stronger at more rapid rotation rates (e.g., Donahue et al., 1996). In our initial exploration of dynamo action in more rapidly rotating stars, we have undertaken simulations which self-consistently establish differential rotation through the coupling of convection and rotation and then explore the resulting dynamo action in the bulk of the convection zone.

2. Global simulations of stellar convection

To capture the essential couplings between convection, rotation and magnetism, we must employ a global model which simultaneously captures the spherical shell geometry and admits the possibility of zonal jets, large eddy vortices and convective plumes which may span the depth of the convection zone, as well as global-scale magnetic structures. Stellar convection zones are intensely turbulent and molecular values of viscous, thermal and magnetic diffusivity in stars are estimated to be very small. As a consequence, numerical simulations cannot hope to resolve all scales of motion present in real stellar convection and a compromise must be struck between faithfully capturing the important dynamics within small regions and capturing the connectivity and geometry of the global scales.

Our tool for exploring stellar dynamos is the anelastic spherical harmonic (ASH) code, which is described in detail in Clune et al. (1999) and with magnetism in Brun et al. (2004). ASH is a mature simulation code, designed to run on massively parallel architectures, which solves the three-dimensional MHD equations of motion under the anelastic approximation. The treatment of velocities and magnetic fields is fully non-linear, but under the anelastic approximation the thermodynamic variables are linearized about their spherically symmetric and evolving mean state with density $\bar{\rho}$, pressure \bar{P} , temperature \bar{T} and specific entropy \bar{S} all varying with radius. The anelastic approximation captures the effects of density stratification but filters out sound waves and the fast magneto-acoustic waves which would severely limit the time step. These acoustic waves are largely decoupled from the decidedly subsonic convective motions in the interior.

With present and foreseeable computational resources, global-scale codes cannot resolve all scales of motion present in real stellar convection zones. With ASH, we explicitly resolve the largest scales of motion and model the transport properties of scales below our resolution. We are thus performing a large eddy simulation (LES) with subgrid-scale (SGS) modelling. The current SGS model treats these scales with effective eddy diffusivities ν , κ , and η , representing the transport of momentum, heat and magnetic field by the unresolved motions. For simplicity these diffusivities are taken as functions of radius alone and in these simulations are proportional to $\bar{\rho}^{-1/2}$.

As we are primarily interested in the coupling of rotation, convection and global-scale flows in the bulk of the convection zone, we avoid the H and He ionization regions near the stellar surface as well as the tachocline of shear at the base of the convection zone. Our simulation extends from $0.72R_{\odot}$ to $0.96R_{\odot}$, with an overall density contrast of 40

across the domain. Solar values are taken for heat flux, mass and radius, and a perfect gas is assumed. The reference state of our thermodynamic variables is derived from a one-dimensional solar structure model (Brun et al., 2002) and is continually updated with the spherically-symmetric components of the thermodynamic fluctuations as the simulations proceed. The simulations reported here are of a star rotating at three times the current solar rate and are derived from hydrodynamic case G3 as reported in Brown et al. (2007), and these dynamo simulations are denoted as case D3. An initial weak dipole field was introduced and over a 1000 day period the simulation amplified the total magnetic energy by several orders of magnitude. The simulation then ran an additional 4000 days in this equilibrated state to explore the long-term dynamo behaviour. The mid-convection zone value of ν is 1.32×10^{12} cm²/s and the Prandtl number $Pr = \nu/\kappa$ is 0.25 while the magnetic Prandtl number $Pm = \nu/\eta$ is 0.5. The ohmic diffusion time at mid-convection zone $\tau_\eta = D^2/\eta$ is approximately 1200 days, with D the depth of the convection zone. Our upper boundary is stress free for velocities and potential field for magnetism. The lower boundary is stress free and a perfect electric conductor. The spatial resolution in these simulations involves using spherical harmonics up to degree 170 or 340 with typically 96 to 192 radial grid points, and the study of the temporal evolution requires close to five million timesteps.

3. Structure of convection

The structure of convective patterns in our more rapidly rotating sun is illustrated in Figure 1. The radial velocity is shown near the top of the domain and at mid-convection zone in Mollweide projection, with poles at top and bottom and the entire equatorial region in the middle. Asymmetries in the convection arise from the density stratification, resulting in narrow, fast downflows surrounded by broad, weaker upflows. Convection in the equatorial region is dominated by large cells aligned with the rotation axis. These convective structures are largely double-celled in radius, owing to the strong radial shear in differential rotation, but strong intermittent downflows span the domain. At high latitudes the convection is more isotropic and cyclonic. At mid-convection zone the Reynolds number of the convection is ~ 170 and the local Rossby number is ~ 0.4 .

The differential rotation is established by Reynolds stresses in the convection. There is a monotonic decrease in local angular velocity from the fast equator to the slow poles (Fig. 1c). Convective enthalpy transport in latitude establishes a prominent latitudinal temperature contrast (Fig. 1d) as convective cells partially align with the rotation axis. This thermal profile is consistent with a thermal wind balance serving to maintain the differential rotation.

4. Strong magnetism amidst turbulent convection

A remarkable finding in these rapidly rotating stellar dynamos is the presence of strong, organized magnetic structures which fill the convection zone and live amidst the turbulent convection. The structure of the toroidal field is illustrated in Figure 2a, b.

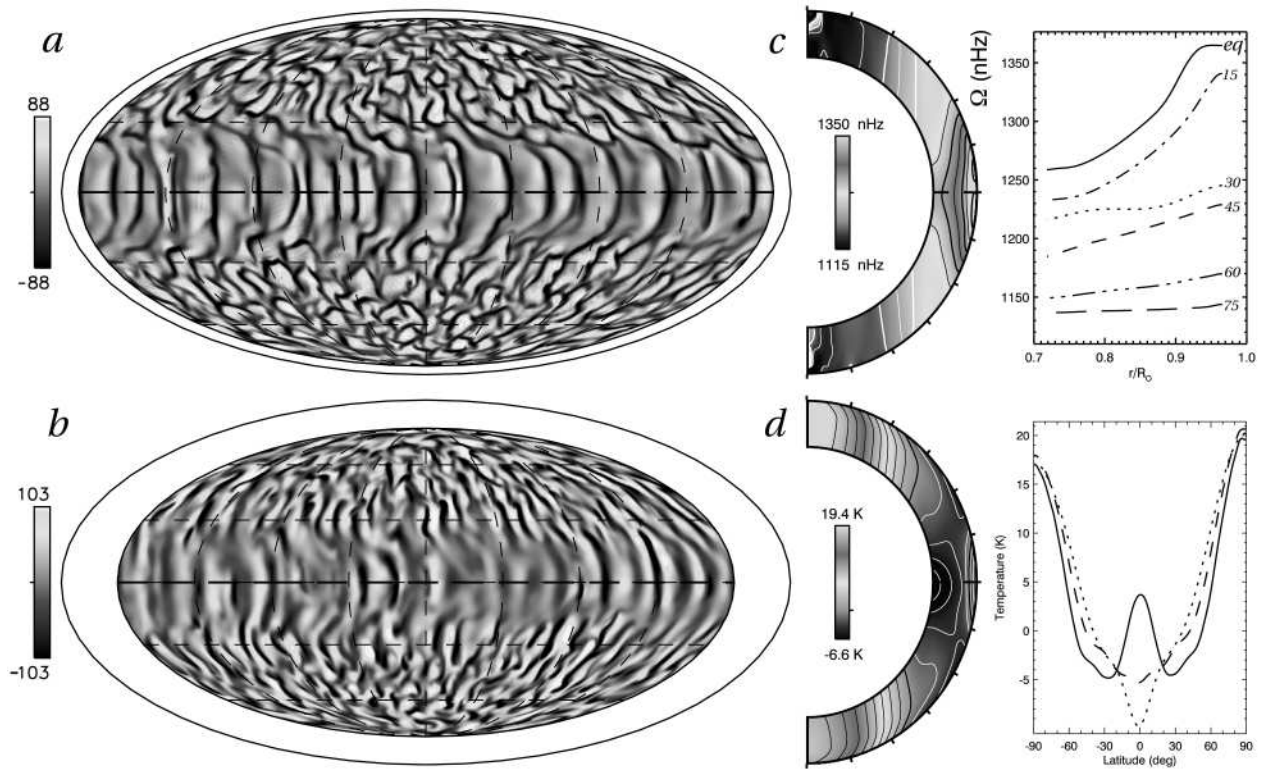


FIGURE 1. Snapshots of radial velocity in global Mollweide view at the same instant in time (*a*) near the stellar surface ($r = 0.95R_{\odot}$) and (*b*) at mid-convection zone ($r = 0.85R_{\odot}$) for case D3. Upflows are denoted by light tones while downflows are dark, with scale in m/s. Strong plumes penetrate to the deepest layers, while weaker plumes are double-celled in radius. (*c*) Azimuthal average of angular velocity Ω with radius and latitude. This has been further averaged in time over a 240 day period. The equator is fast and the poles are slow. Plotted at right are radial cuts of Ω at selected latitudes as indicated. (*d*) Azimuthal and time average of temperature fluctuations T' about the spherically symmetric mean \bar{T} . The poles are warm and the equator largely cool. Plotted at right are three cuts in latitude near top ($r = 0.96R_{\odot}$, solid, with $\bar{T} = 2.7 \times 10^5$ K), middle ($r = 0.85R_{\odot}$, long dash, with $\bar{T} = 1.1 \times 10^6$ K) and bottom of the convection zone ($r = 0.72R_{\odot}$, short dash, with $\bar{T} = 2.3 \times 10^6$ K). Although distinctive, the latitudinal temperature contrast of order 20K is but a very small fraction of the spherically-symmetric mean temperature.

At mid-convection zone, large magnetic domains of each polarity appear near the equator. The magnetic fields in these “sea-snakes” are quite strong, with peak amplitudes over 20kG. The mean toroidal fields are also quite strong, with typical strengths of ± 5 kG and peak amplitudes of ± 15 kG. This is in contrast to previous solar simulations with ASH (Brun et al., 2004) where the magnetic fields were dominated by fluctuating components and the mean fields were quite weak. In the solar case our simulations have required a tachocline of penetration and shear (Browning et al., 2006) to generate similarly ordered toroidal structures. Here we have no tachocline and the fields are generated in the bulk of the convection zone. The sea-snakes of case D3 are quite long lived, persisting for thousands of days despite the turbulent convection. The average poloidal fields are much weaker than the toroidal fields, with typical strengths of ± 3 kG and peak amplitudes of ± 6 kG. The global field has prominent dipolar and quadrupolar compo-

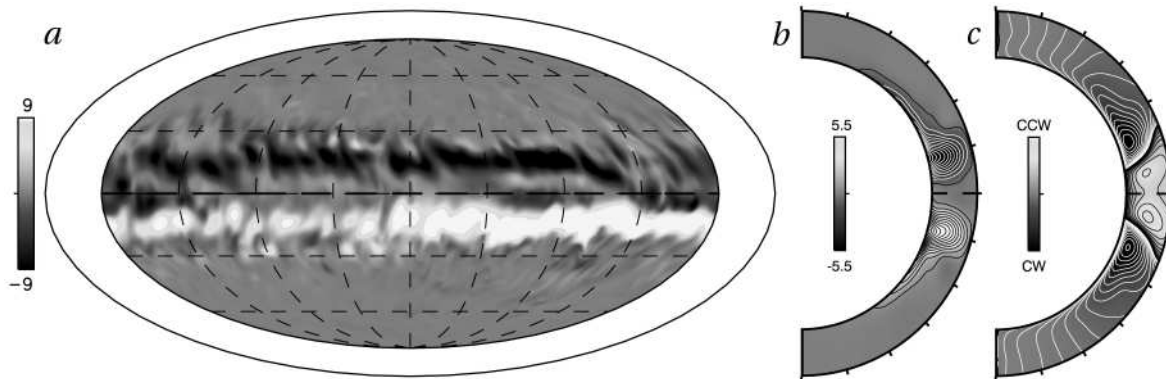


FIGURE 2. Structure of magnetic field for case D3: (a) Snapshot of B_ϕ in Mollweide view at mid-convection zone ($r = 0.85R_\odot$) with scale in kG, at the same instant as in Figure 1a,b. Strong magnetic domains have formed in the midst of the turbulent convection, possessing mainly opposite polarity in the two hemispheres. (b) Azimuthally averaged B_ϕ (scale in kG), with radius and latitude. This has been further averaged over a period of 200 days. The sea-snakes of magnetic field evident in (a) are present throughout the convection zone, with strongest average magnetic field amplitudes ($\sim 15\text{kG}$) near the base of the convection zone. (c) Average poloidal magnetic field lines, showing the global structure of the mean field with polarity of field indicated (light tones counter-clockwise, dark tones clockwise). The peak average amplitude of the poloidal field is about 6.5kG at the base of the convection zone.

nents, as shown in Figure 2c. The mean poloidal and toroidal fields are relatively steady in time and this dynamo shows no cyclic behaviour or oscillations in differential rotation and magnetism.

The three-dimensional structure of the magnetic field is rich and complex (as shown in Fig. 3). The sea-snakes are dominantly toroidal field, but fields thread in and out of these structures and connect to the higher latitudes. Strong downflows kink the sea-snakes in many locations, dragging field to the base of the convection zone before it rejoins the larger structure. Some magnetic fields span across the equatorial region, connecting the two zones of opposite polarity.

After the dynamo has saturated, the total volume-averaged kinetic energy density of motions relative to the rotating reference frame is about $7.15 \times 10^6 \text{ ergs cm}^{-3}$. Much of this is contained in the mean differential rotation which comprises about 69% of the total. Fluctuating convective motions contain almost 31% of the total and meridional circulations are a minor component. The total volume-averaged magnetic energy density is about 11% of the kinetic energy density. Of this, 48% is contained in the mean toroidal fields, 47% in the fluctuating fields and about 5% in the poloidal fields.

5. Cyclic behavior amidst stronger turbulence

Our current models are far in parameter space from the levels of turbulence realized in the convection zones of real stars. A natural question therefore is what occurs as we drive these turbulent solutions to even higher levels of complexity. Are stronger magnetic fields generated? Do the persistent magnetic structures found in the equatorial regions

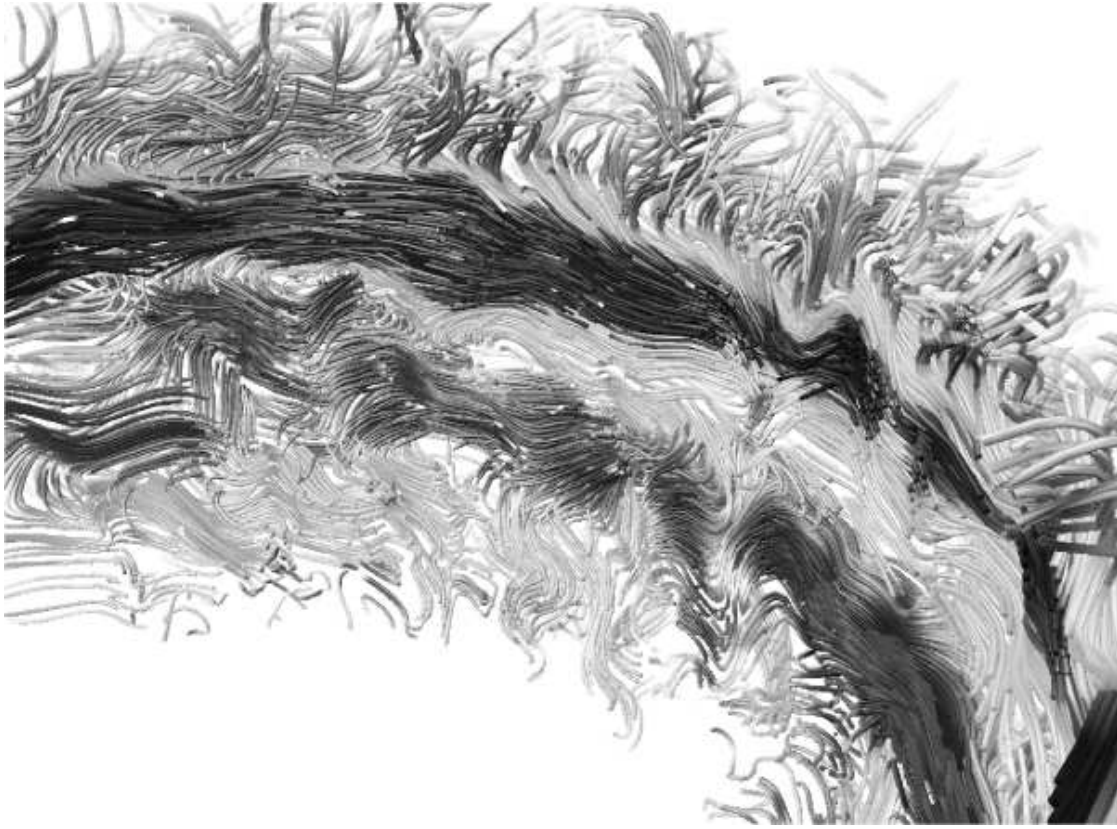


FIGURE 3. Volume rendering of magnetic fields filling the bulk of the convection zone in case D3, showing that these flux concentrations are complex, with field lines threading in and out of the concentrated regions. The view is from the center of the star and directed towards the surface, and occupies a region near the equator that spans from $\pm 45^\circ$ in latitude. The two regions of strong opposite polarity (dark tones) above and below the equator are largely toroidal field, while the weaker fields reaching towards the polar regions have been twisted by the vortical convection.

survive the more vigorous turbulence?

To begin addressing these questions we have conducted a second dynamo simulation for a similar star rotating three times the solar rate but with lower levels of eddy diffusivities and therefore higher levels of convective turbulence. The diffusivities in our original dynamo case D3 were dropped by about 30% to a new mid-convection zone value of ν of $0.94 \times 10^{12} \text{ cm}^2/\text{s}$, while maintaining a Prandtl number of 0.25 and a magnetic Prandtl number of 0.5. The new solution, case D3a, has a mid-convection Reynolds number of ~ 230 and a local Rossby number of ~ 0.45 .

An intriguing result from this simulation is that the dynamo has achieved a new state, wherein oscillations in energy and magnetic field structure occur over time scales which are long in comparison to characteristic convective turn-over times or the stellar rotation rate, as is illustrated in Figure 4. The kinetic energy in differential rotation undergoes similar long-period oscillations, whereas the kinetic energy in convection and the meridional circulations is nearly unaffected. The structure of the magnetic fields is similar to case D3, with two strong sea-snakes of opposite polarity above and below

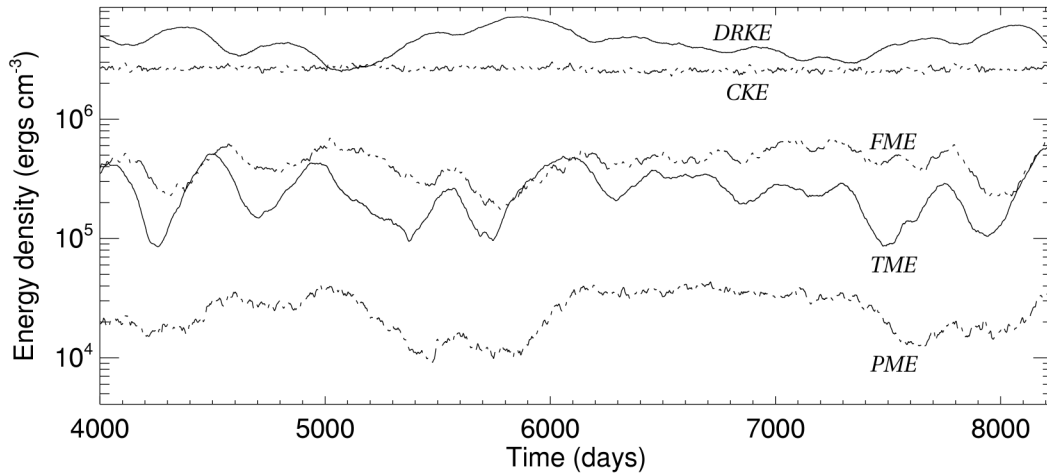


FIGURE 4. Volume averaged energy densities late in case D3a. Shown are kinetic energies in differential rotation (DRKE) and convection (CKE) as well as magnetic energies in mean toroidal fields (TME), mean poloidal fields (PME) and in the fluctuating fields (FME). Oscillations between kinetic energy and magnetic energies occur, with DRKE and PME moving oppositely over long periods and TME and FME moving largely together on shorter timescales.

the equator. With the oscillations in magnetic energy, the sea-snakes wax and wane in strength, sometimes synchronously and sometimes individually, with one polarity growing and one fading.

The total kinetic energy relative to the rotating reference frame is somewhat lower in this simulation, with a volume and time average of 6.82×10^6 ergs cm^{-3} over the 4200 day period shown in Figure 4. Mean differential rotation accounts for 60% of this, while convection accounts for nearly 40%. The time averaged total magnetic energy is about 11% of the kinetic energy, with mean toroidal fields accounting for about 33% of the total magnetic energy and fluctuating fields comprising nearly 63%. There are intervals where the sense of the large-scale toroidal fields nearly flips, but then the fields regain strength while retaining their original sense.

6. Global dynamos without a tachocline

A surprising result of these simulations of rapidly rotating stars is that global-scale toroidal and poloidal magnetic fields can be built and maintained in the bulk of the convection zone, despite the presence of turbulent convective motions, without resorting to a stable tachocline of shear which stores and combs out the large-scale fields. For the solar dynamo, it has long been thought that the turbulence of the convection zone precludes the existence of globally organized fields there. Instead, we have arrived at the theoretical concept of an interface dynamo (Parker, 1993) in which fluctuating fields arise from dynamo action in the convection zone, and these are then pumped into the tachocline where gradually global-scale fields are built and organized. Indeed, previous

ASH simulations of solar dynamo action in the bulk of the convection zone (Brun et al., 2004) built mostly fluctuating fields with little global-scale structure. Organized, global-scale toroidal fields have only emerged in solar simulations where a tachocline has been included (Browning et al., 2006). These simulations of rapidly rotating solar-like stars represent the first time to our knowledge when organized structures have been built and maintained amidst vigorous, three-dimensional turbulent convection in the bulk of the convection zone.

These simulations suggest that dynamo action in rapidly rotating stars may yield global-scale fields even without resorting to an interface dynamo. This latter dynamo crucially requires a boundary layer of strong radial shear to comb the fields into strong toroidal structures. Yet with more rapid rotation this seems to be no longer necessary. This may have important implications for fully convective stars in which no such interface exists. The sea-snakes of toroidal field arising in the current simulations are able to freely rise through our upper boundary, yet they remain strong and fill the convection zone. The pumping action of convective downflows near the equator must effectively resist the magnetic buoyancy which otherwise would lead to these fields escaping the domain. The behavior exhibited here is changing our intuition of the dynamo action that can be realized in stars with rapid rotation. A crucial question for the future is whether these organized magnetic structures survive in the convection zone in the presence of a penetrative tachocline

This research was supported by NASA through Heliophysics Theory Program grant NNG05G124G and the NASA GSRP program by award number NNG05GN08H. The simulations were carried out with NSF PACI support of PSC and SDSC.

REFERENCES

- Brown B. P., Browning M. K., Brun A. S., Miesch M. S., Toomre J., 2007, ApJ, submitted
Browning M. K., Miesch M. S., Brun A. S., Toomre J., 2006, ApJ, 648, L157
Brun A. S., Antia H. M., Chitre S. M., Zahn J.-P., 2002, A&A, 391, 725
Brun A. S., Miesch M. S., Toomre J., 2004, ApJ, 614, 1073
Charbonneau P., 2005, Living Reviews in Solar Physics, 2, 2
Clune T. L., Elliott J. R., Glatzmaier G. A., Miesch M. S., Toomre J., 1999, Parallel Computing, 25, 361
Donahue R. A., Saar S. H., Baliunas S. L., 1996, ApJ, 466, 384
Parker E. N., 1993, ApJ, 408, 707
Thompson M. J., Christensen-Dalsgaard J., Miesch M. S., Toomre J., 2003, ARA&A, 41, 599